Proceedings of the 2012 Industrial and Systems Engineering Research Conference
G. Lim and J.W. Herrmann, eds.

Modeling of Multifunctional Deformable Porous Scaffolds for Soft Tissue Engineering

AKM Khoda[1] and Bahattin Koc [1,2]

[1]Department of Industrial Engineering, University at Buffalo, Buffalo, NY 14260, USA
[2]*Faculty of Engineering and Natural Sciences, Sabanci University, Istanbul 34956, Turkey*

Abstract

Porous membranes/scaffolds such as guided tissue regeneration (GTR) membranes, cell sheets, tissue matrices or polymeric meshes are being widely used in soft tissue engineering to regenerate damaged, diseased tissue or wound. These membranes are mostly regular porous structures with repeating internal architecture. When they are applied onto wound area, various forces caused by bandage, contraction and self weight might cause deformation. As a result, the geometry and the designed porosity changes which eventually alters the desired choreographed functionality. To avoid the negative effect cause by such deformation and its associated consequences, a novel design methodology has been proposed to determine and include the resultant deformation. The proposed design will minimize the variation in effective porosity while ensuring its surface conformity. Thus the proposed design will provide a better functionality by providing both structural integrity and proper biological properties. The proposed methodology has been implemented and results will be shown with illustrative examples. Also a comparison study showing effective porosity for both the proposed method and conventional regular porosity will be presented for a free-form surface mimicking a wound.

Keyword:

Keywords

Scaffold design, deformed scaffold, soft tissue engineering.

1. Introduction

Scaffold structure is being commonly used as a conduit to deliver bio-molecules (usually cytokines) and/or cells into the targeted region for tissue engineering applications. This could induce amenable bio-reactor to stimulate the regeneration process by protecting the seeded cell against host immunorejection [1]. In many instances, such scaffold structures are often designed as bi-layers and homogeneous porous membranes in the form of wound dressing and/or drug delivery modules [2]. Other than biodegradability, biocompatibility, non-cytotoxicity and non-antigeneticity [2], they must have physical agility (e.g. pliability, elasticity) [3] for proper adherence, ease of application and removal and avoid wrinkling or fluting [4]. But when applied in the wound area, various forces may act upon the membrane which might be generated from bandage or occlusive dressing [5], contraction due to vacuum assisted wound closure (VAC) [6], curvature of the skin, and/or self weight. These forces could deform the visco-elastic membrane as shown in Figure 1. As a result, the geometry and the designed porosity would change which eventually alter the vital characteristics such as material concentration, design parameters and cytokines distribution over the wound device geometry. This could jeopardize the choreographed functionality affecting the wound environment, triggering inflammatory response and reversing the wound healing process.

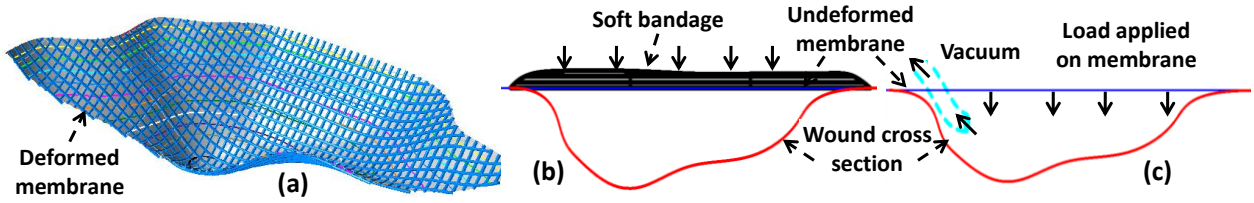

Figure 1: (a) shape conforming deformation of a uniform porous membrane; (b-c) Schematic diagram showing the load applied on the membrane from dressing.

In this paper, we evaluate the affect of deformation of a membrane/dressing on its resultant porosity. The porosity is a critical factor for the device functionality and such deformation alter the designed material concentration/porosity and might have adverse affect on the wound micro environment. To avoid such effect, a novel scaffold modeling has been proposed based on the free-form wound surface geometry that will minimize the difference between the designed and the effective porosity. Thus the proposed method will give a better functionality of such membrane providing predictable material concentration along the wound surface. The proposed methodology has been implemented in this paper and the illustrative example has been provided via a computer simulation. To measure the effectiveness of the proposed model, the shape conforming deformation has been modeled with a finite element analysis method (Abaqus 6.9) using the commonly used hydrogel properties. To illustrate, a virtual bi-layer membrane has been applied on a free-form surface mimicking wound and the resultant porosity has been measured and compared for both the proposed design and the conventional design.

The rest of the paper is organized as follows. Section 2 evaluates the deformation effect on the conventional equidistant membrane. Section 3 discussed the proposed "desired porosity with variational filament distance" methodology for better control. The proposed design has been implemented with a free-form virtual wound shape and the results have been shown in Section 4. And finally, we draw conclusions in Section 5.

2. Deformed Porosity for Homogeneous Membrane

To explain the shape conforming deformation in a traditional equidistant filament structure, two adjacent filaments of a single layer have been considered as shown in Figure 2. Based on the geometry, the volume covered by a single layer can be discretized into segments, where R_1 is the filament radius, W_1 is the segment width and L_1 is the distant between filaments. Thus the porosity in each segment is the same and can be calculated by the following equation,

$$Porosity_{Seg} = \frac{V_{seg} - V_{fil}}{V_{seg}} \times 100\% \tag{1}$$

Here, V_{seg} is the segment volume and V_{fil} is the filament volume in each segment. For such homogeneous layer, the designed porosity is directly correlated with the filament diameter and the segment size. Any changes in the design parameter would result in a deviation from the desired porosity. Now the load on the scaffold creates deformation and the membrane will conform to the shape of the wound surface under applied force due to its visco-elastic property. Such shape conforming deformation would affect both the design parameters which eventually change the effective porosity of the membrane or the scaffold.

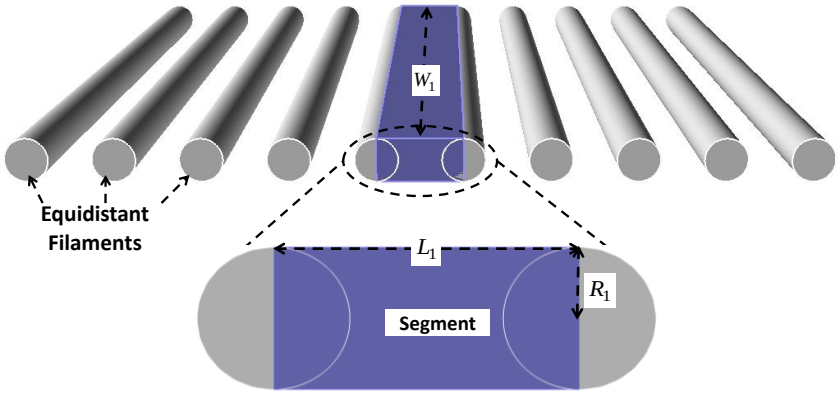

Figure 2: Equidistant cylindrical filaments with designed porosity.

Considering only a single filament with initial length W_1, it can be assumed as two end supported beam. Due to the applied load, it will go through strain and thus the filament will be elongated according to the material properties and the deformed length become W_2 , where $W_2 > W_1$ as shown in Figure 3.

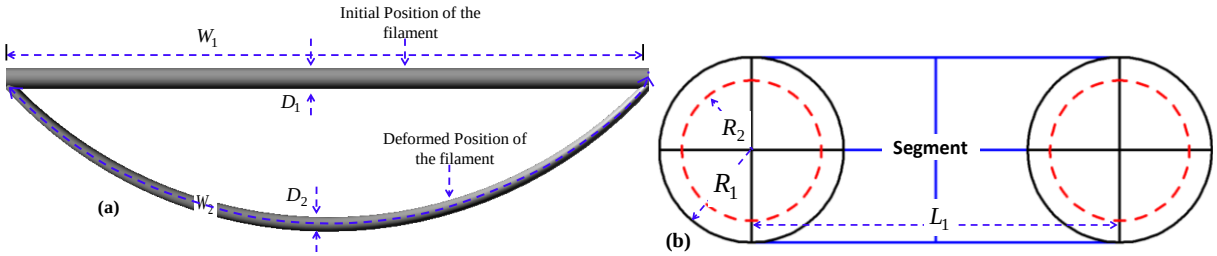

Figure 3: Change in filament (a) length and (b) corresponding diameter due to the deformation.

By assuming uniform filament diameter for both deformed and undeformed filament and by applying the volume conservation principle, the deformed porosity in each segment can be calculated by the following equation [2].

$$Porosity_{Def\_Seg} = (1 - \frac{\pi R_1}{2L_1} \mathrm{Cos}\phi_{avg}) \times 100\% \qquad \forall\, 0^0 < \phi_{avg} < 90^0 \tag{2}$$

Thus, the resultant porosity increases following the slope of the wound surface which implies the deformation depth. Now, this single segment deformed porosity model can be mapped for membrane placed over a free-form wound shape. And thus by using this relationship presented in Equation (2), the proper design parameters can be selected to eliminate or minimize the deformation effect on the porosity. Also, in Equation (2) ϕ_{avg} depends upon the wound profile and can be considered as uncontrollable parameter. R_1 is the radius of the undeformed filament which depends upon the fabrication capability and can be considered as fixed. Similarly, R_2 is the deformed filament radius. Hence the proposed methodology determines the adjusted distance between the filaments, $L_1^{/}$ to achieve the desired porosity.

3. Designing Controllable Porosity in Bi-layer Membrane

3.1 Slicing the Model and Generating Strips

To counteract the deformation effect on the membrane which results in non-uniform material concentration on the wound surface, a novel method has been proposed to determine the adjusted distance between the filaments.

Firstly, medical image obtained from Computed Tomography (CT), Magnetic Resonance Imaging (MRI) or reverse engineering is used to obtain the geometric and the topology information of the wound shape. The 3D wound model

is then converted to the STL file format using a CAD system's converter and sliced by a set of intersecting planes perpendicular to the depth of the surface to find the slicing contours $S = \{s_i\}$, where i is the number of contour slice for the wound geometry. The contours are generated by connecting the intersection points between the plane and the surface. The distance between the intersecting planes can be constant in uniform slicing i.e $h_i = h \ \forall i$ or varying height $h_i \neq h \ \forall i$ and can be identified as a controllable design parameter as shown in Figure 4. These height/ depth specified sliced contours are then projected as a set of projected contours $P_s = \{P_{s_i}\}$ on the wound top-plane and a set of parallel lines $SL = \{SL_j\}$ have been drawn along the lay-down direction to discretize those projected contours. The distance between such intersecting lines can be uniform $d\_SL_i = d\_SL_j \ \forall i, j$ or variational $d\_SL_i \neq d\_SL_j \ \forall i, j$ and must be greater than the width of a single segment, $d\_SL_i > \text{Segment\_width} \ \forall i$ is shown in Figure 2. The area generated between two adjacent parallel lines has been noted as strips $ST = \{ST_{j+1}\}$ and the effective area for k^{th} strip can be defined as the area generated by the outer most projected contour in that strip i.e. $ST_k^{eff} = \{ST_k \cap P_{S_{i=S}}\}$ as shown in Figure 4(b).

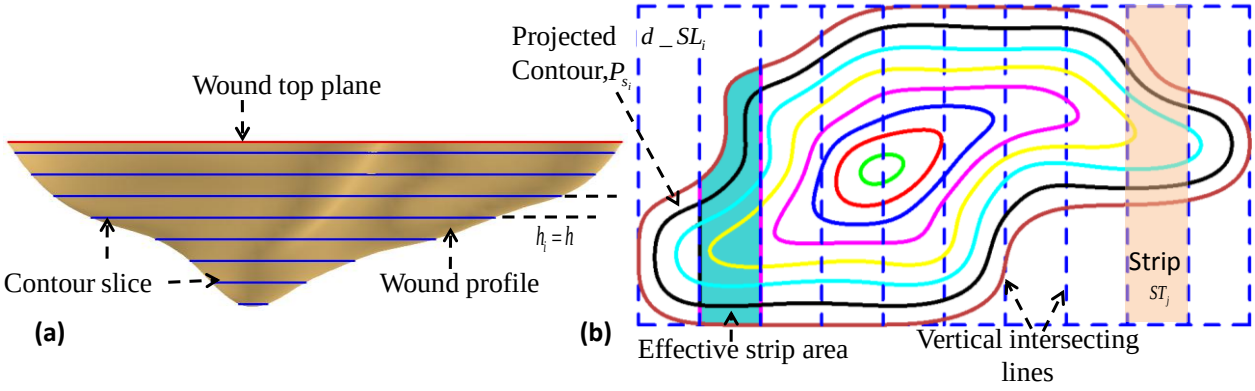

Figure 4: (a) Generating height base contour (b) strips.

Both the number of height/ depth specified sliced contour and the number of strips can be considered as controllable design parameters which can be represented as quadratic function for wound surface approximation and can be represented by the following equation.

$$\alpha L \leq (d\_SL + h) \leq \beta L \quad \forall \ 1 < \alpha \leq \beta \tag{3}$$

Where, the two controllable parameters i.e. strip width, d_SL and slice distance, h have been combined $(d\_SL + h)$ together. The two uncontrollable parameter i.e. porosity and filament radius have been replaced by a single parameter L i.e. distance between filament in conventional membrane. L can be calculated by using Equation 2 with $\phi_{avg} = 0^0$. α and β are the constants that determine the upper and lower range of the combined controllable parameters based on the remaining uncontrollable parameters. For a complex wound surface, the value of $(d\_SL + h)$ should be on the lower range and vice versa.

3.2 Strips Surface Normal and Corresponding Filament Distance

To approximate the free form wound surface profile with three dimensional point location, a contour area based average surface normal angle determination methodology [2] has been applied where the set of slicing contour S from previous section act as guiding contours.

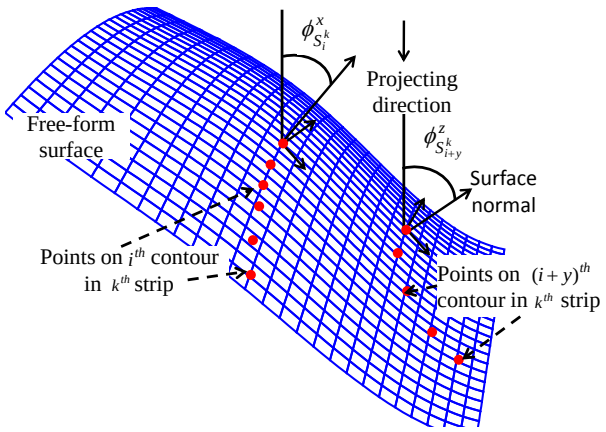

Figure 5: Measuring the surface normal along the projected contour and wound profile.

If k^{th} strip has intersection with n_k number of projected contour, then the resultant surface normal for that strip, can be calculated by the following equation,

$$\phi_{avg}^{k} = \left(\sum_{i}^{n_k-1} \left|\phi_{S_i^k}\right|_{eff} \times \frac{P_{S_i}^{k} - P_{S_{i+1}}^{k}}{ST_k^{eff}}\right) + \left(\left|\phi_{S_{n_k}^k}\right|_{eff} \times \frac{P_{S_{n_k}}^{k}}{ST_k^{eff}}\right) \qquad \forall\ k \tag{4}$$

$$\left|\phi_{S_i^k}\right|_{eff} = \frac{\sum_{x=1}^{N_i^k} \phi_{S_i^k}^{x}}{N_i^k = \left(\frac{P_{S_i}^{k} - P_{S_{i+1}}^{k}}{ST_k^{eff}}\right) \times n} \qquad \forall \quad i,\ k \tag{5}$$

Where, ϕ_{avg}^{k} is the average surface normal angle of k^{th} strip, $\left|\phi_{S_i^k}\right|_{eff}$ is the effective average surface normal angle measured on i^{th} contour section fall in k^{th} strip calculated by the Equation 5, $P_{S_i}^{k}$ is the area generated by i^{th} projected contour section fall in k^{th} strip, N_i^k is the number of points on the i^{th} contour section fall in k^{th} strip. N_i^k has been determined rationally based on the percentage area of i^{th} contour in k^{th} strip. n is a integer and can be defined as resolution for ϕ_{avg}^{k}. Finally by determining the surface normal angle for each strip, the distance between filaments in individual strip can be determined by using Equation 6 that could counteract the change in material concentration due to the deformation.

$$L_1^k = \frac{\pi R_1}{2(1 - Porosity_{Desired})} Cos\phi_{avg}^{k} \tag{6}$$

Where, L_1^k is the space between fibers in k^{th} strip, R_1 is the deposited filament radius which depends upon fabrication system capability, $Porosity_{Desired}$ is the desired porosity level in the membrane. Determining the filament distribution distance for all the strips, the filament deposition location for the first layer is completed. The same methodology has been applied for consecutive layer using strips parallel to the filament lay-down pattern. All the design parameters discussed earlier are layer independent design parameters.

3.3 Analyze and Evaluation of the Designed Membrane

Due to the free-form wound surface and the shape conforming deformation, the resultant parameters for each deformed filament become distinct and thus segment concept or the unit pore-cell concept no longer prevails. Thus quadrilateral pore-cell concept [7] is more appropriate for measuring the porosity that combine consecutive layers as shown in Figure 4. Because of the free form wound shapes, the generated quadrilateral pore-cells are highly anisotropic in nature. And due to this variation, the porosity in each pore-cell needs to be measured by using the following equation.

$$Porosity_{i,i+1,j,j+1}^{porecell} = 1 - \frac{\pi(R_2^{i\,2} A_4 + R_2^{j\,2} A_3 + R_2^{i+1\,2} A_2 + R_2^{j+1\,2} A_1)}{Area\_A_1A_2A_3A_4 \times 8 \times R_1} \qquad \forall\ i, j \tag{7}$$

Where, $Porosity_{i,i+1,j,j+1}^{porecell}$ is the porosity of the pore-cell generated by i^{th} and $(i+1)^{th}$ filament of first layer and j^{th} and $(j+1)^{th}$ filament of consecutive layer. R_2^i, R_2^{i+1}, R_2^j and R_2^{j+1} are the deformed radius for i^{th}, $(i+1)^{th}$, j^{th} and $(j+1)^{th}$ filament respectively. Also, A_1 is the segment length of $(j+1)^{th}$ filament falls between i^{th} and $(i+1)^{th}$ filament of first layer as shown in the following Figure 6(a). Similarly, A_2, A_3 and A_4 are the segment of $(i+1)^{th}$, j^{th} and i^{th} filament respectively.

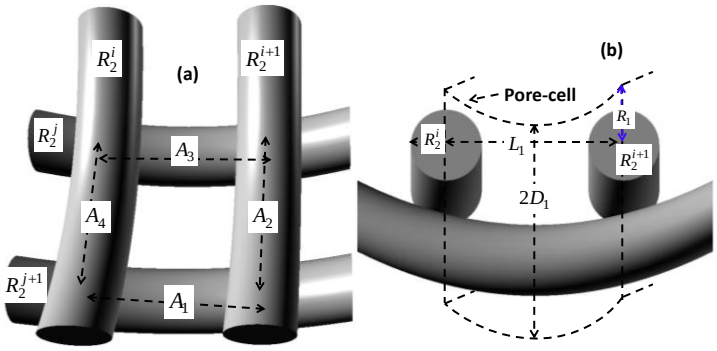

Figure 6: Pore-cell and deformed porosity calculation.

To quantify the effectiveness of the proposed method, a percentage area based porosity evaluation index (PPEI) has been used [2] as follows:

$$PPEI = \sum_{-i}^{i} \frac{CellArea\_Porosity_{DP(1+ni)\sim DP(1+n(i+1))}}{Wound\_Area} \times \frac{|ni| + |n(i+1)|}{2} \qquad \forall\ i:\ i \in \mathbf{Z},\ n > 0 \tag{8}$$

Where, DP is the desired porosity, n is the percentage increment factor, $CellArea\_Porosity_{DP(1+ni)\sim DP(1+n(i+1))}$ is the total surface area of the deformed pore-cell that has resultant porosity within the $DP(1+ni) \sim DP(1+n(i+1))$ range and $Wound\_Area$ is the wound surface area, $\frac{|ni| + |n(i+1)|}{2}$ is the penalty factor which is proportional to the resultant porosity deviation.

4. Implementation

The proposed methodology has been implemented to a non-convex free-form surface profile mimicking as a virtual wound shape as shown in Figure 5. The model has been generated by using NURBS based Rhino 4.0. The contour line shows the free-form surface profile along its depth which is taken 0.6 mm apart. The maximum depth for this generated surface is 6.7 mm which is shown in Figure 7. The maximum width and length is 16 mm and 30 mm respectively. A two layers 0^0-90^0 layout pattern membrane with constant porosity has been generated by both the conventional and the proposed design methods using Rhinoceros 4.0 and Visual-Basic language. The membranes are placed over the generated virtual wound surface and uniform axial load has been applied on them to mimic the dressing load which might cause shape deformation of the membranes. The deformation has been modeled in Abaqus 6.9 by using the hydrogel bio-material properties. Then the deformed membranes are used for porosity analysis by applying the methodology described in Section 3. A color legend surface has been used to visualize the resultant porosity comparison in both the conventional and the proposed membrane designs.

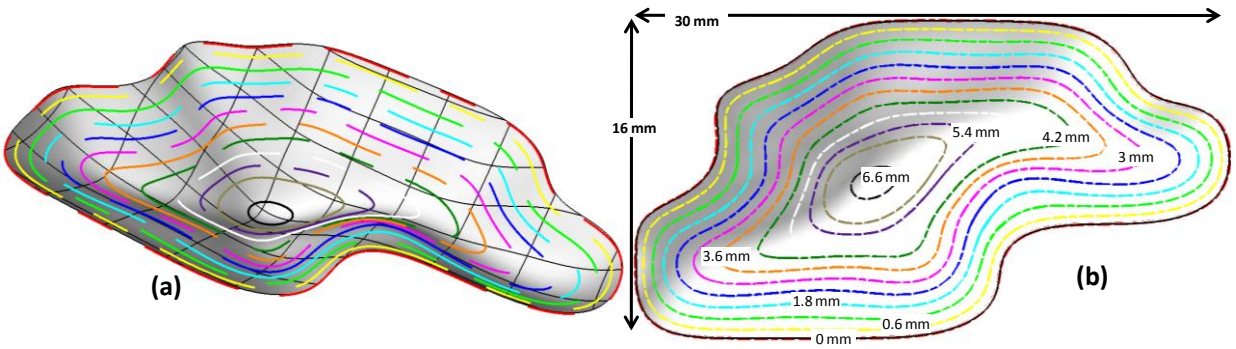

Figure 7: (a-b) A free form shape and its contour along the depth shows non-symmetry along every directions.

A shape conforming deformation for both the proposed and the conventional designed bi-layer hydrogel membranes have been modeled on this free-form surface using Abaqus 6.9 as shown in Figure 8. Then the deformed FEA model geometry profiles (Figure 8(b)) have been transferred to Rhinoceros 4.0 for analyzing the deformed porosity as discussed in section 2.3.

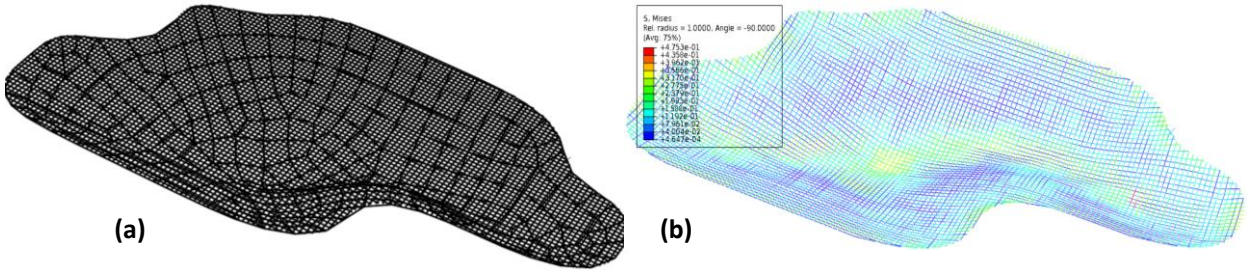

Figure 8: (a) The undeformed mesh model of both virtual surface and bi-layer membrane for FEA analysis (b) deformed bi-layer membrane with stress profile generated by FEA (Abaqus 6.9).

Table 1. Converging parameter for the free-form surface presented in Figure 7.

% Designed Porosity, P	**Filament Diameter,** D **mm**	$L=\frac{\pi D}{4(1-P)}$ **, mm**	**Proposed method**					**Conventional Method PPEI**
			Vertical Strip Number	**Horizontal Strip Number**	**Slice Distance,** h **mm**	d_SL+h	**PPEI**	
55	**100**	**0.174**	**30**	**16**	**0.5**	**8.6** L	**7.92**	**12.74**
			60	**32**	**0.5**	**5.75** L	**6.23**	
			60	**32**	**0.3**	**4.6** L	**7.53**	
			42	**23**	**0.2**	**5.2** L	**4.25**	
			60	**32**	**0.3**	**4.6** L	**6.78**	

A computer simulated deformation analysis has been performed based on the desired porosity of 55% and filament diameter of 100 µm by changing the controllable parameters to achieve convergence as shown in Table 1. All these models perform better than the conventional equidistant method and the convergence has been achieved at $(d\_SL+h)=5.2L$.

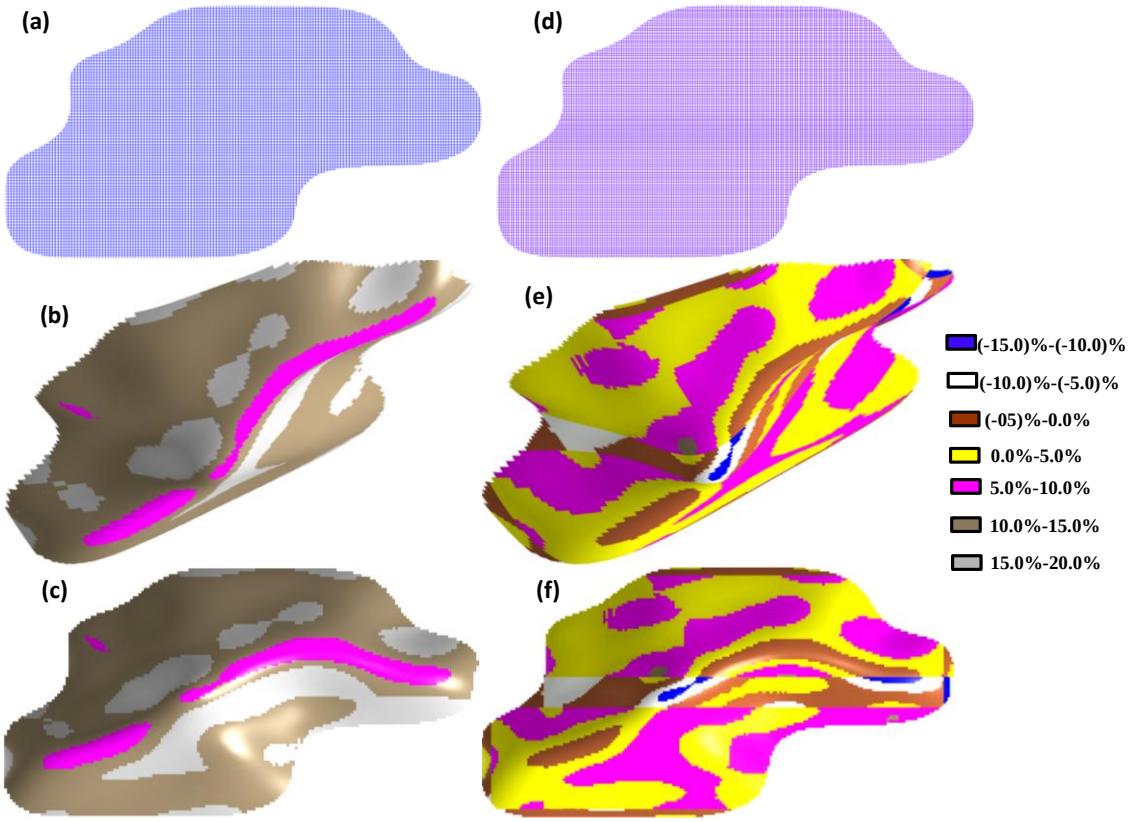

Figure 9: Porosity comparison on two layer membrane with 55% porosity and 50 µm filament radius (a & c) designed filament; and deformed porosity (b & d) perspective view (c & f) top view for conventional fixed filament distance and proposed variational filament distance respectively (color legend represent the % deviation from the designed porosity).

In the conventional equidistant filament method, 55% porosity requires 91 horizontal filaments and 172 vertical filaments with radius of 50 µm. On the other hand the proposed method for variational distance requires 104 and 201 filament respectively. In the case of conventional membrane, 61.4% of its area shows 10%-15% higher porosity and 26% of its area shows 15%-20% higher porosity than the designed porosity (55%). But by using the proposed method for the same surface, a total 58.5% of its surface area has a resultant porosity within ±5% and 31.4% area shows 5%-10% higher porosity than designed porosity as shown in Figure 9 which is significantly low from its counterpart.

5. Conclusion

In this research, the effect of membrane deformation on its designed porosity has been analyzed. Due to the deformation, a significant change in resultant porosity in the membrane has been observed. The deformation should be factored and incorporated during the membrane design for an effective tissue regeneration. A novel 'desired porosity with variational filament distance' methodology has been proposed to eliminate/reduce the deformation effect and to minimize the difference between the actual and the designed porosity on the multi-functional membrane. The difference in the deformed and the desired porosity may not be eliminated completely for free form complex surfaces, but this proposed modeling technique would provide better control to achieve the desired porosity over the scaffold structure spatially.

References

[1] Levenberg, S., and Langer, R., 2004, "Advances in Tissue Engineering," Current Topics in Developmental Biology, P. S. Gerald, ed., Academic Press, pp. 113-134.

[2] Khoda, A., and Koc, B., 2011, "Deformable Porosity for Multi-Functional Tissue Scaffolds," ASME Transactions, Journal of Medical Device (Submitted).
[3] Hong, H., Dong, G. N., Shi, W. J., Chen, S., Guo, C., and Hu, P., 2008, "Fabrication of Biomatrix/Polymer Hybrid Scaffold for Heart Valve Tissue Engineering in Vitro," ASAIO Journal, 54(6), pp. 627-632 610.1097/MAT.1090b1013e31818965d31818963.
[4] Balakrishnan, B., Mohanty, M., Umashankar, P. R., and Jayakrishnan, A., 2005, "Evaluation of an in situ forming hydrogel wound dressing based on oxidized alginate and gelatin," Biomaterials, 26(32), pp. 6335-6342.
[5] Eaglstein, W. H., 2001, "Moist Wound Healing with Occlusive Dressings: A Clinical Focus," Dermatologic Surgery, 27(2), pp. 175-182.
[6] SAXENA, #160, Vishal, HWANG, Chao-Wei, HUANG, S., EICHBAUM, Quentin, INGBER, Donald, ORGILL, P., D., LOHMAN, F., R., LEE, and C., R., 2004, Vacuum-assisted closure: Microdeformations of wounds and cell proliferation. Discussion, Lippincott Williams & Wilkins, Hagerstown, MD, ETATS-UNIS.
[7] Khoda, A., Ozbolat, I. T., and Koc, B., 2011, "A functionally gradient variational porosity architecture for hollowed scaffolds fabrication," Biofabrication, 3(3), pp. 1-15.